

PAPER

Experimental simulation of violation of the Wright inequality by coherent light^{*}

To cite this article: Feng Zhu *et al* 2017 *Chinese Phys. B* **26** 100302

View the [article online](#) for updates and enhancements.

Related content

- [Exhibition of Monogamy Relations between Entropic Non-contextuality Inequalities](#)
Feng Zhu, Wei Zhang and Yi-Dong Huang
- [All-or-Nothing-Type Kochen-Specker Experiment with Thermal Lights](#)
Song Xin-Bing, Wang Hai-Bo, Xiong Jun *et al.*
- [A proof of the Kochen–Specker theorem can always be converted to a state-independent noncontextuality inequality](#)
Xiao-Dong Yu, Yan-Qing Guo and D M Tong

Recent citations

- [Detecting Quantumness in the \$n\$ -cycle Exclusivity Graphs](#)
Jie Zhou *et al*

Experimental simulation of violation of the Wright inequality by coherent light*

Feng Zhu(朱锋), Wei Zhang(张巍)[†], and Yidong Huang(黄翊东)

Tsinghua National Laboratory for Information Science and Technology, Department of Electronic Engineering, Tsinghua University, Beijing 100084, China

(Received 21 January 2017; revised manuscript received 23 June 2017; published online 20 August 2017)

In this paper, we investigate the simulation of violation of the Wright inequality by the classical optical experiment theoretically and experimentally. The feasibility of the simulation is demonstrated by theoretical analysis based on descriptions of the classical electrodynamics and quantum mechanics, respectively. Then, the simulation of violation of the Wright inequality is realized experimentally. The setup is based on a laser source, free-space optical devices and power meters. The experimental result violates the noncontextuality hidden variable bound, agreeing with the quantum bound. This method can be extended to other types of noncontextuality inequalities.

Keywords: quantum optics, polarization, quantum information and processing

PACS: 03.65.Ta, 03.65.Ud, 03.67.-a

DOI: 10.1088/1674-1056/26/10/100302

1. Introduction

Quantum mechanics is counterintuitive and its completeness is doubted under assumptions of reality and locality.^[1] An intuitive explanation of the quantum phenomenon is the local hidden variable (LHV) theory.^[2] LHV theory is a special case of a more general theory, which is the noncontextuality hidden variable (NCHV) theory.^[3–5] In NCHV theory, outcomes of the measurement in a physical system are predetermined and depend on the hidden variable λ . The distribution of the outcomes comes from the statistical characteristics of λ . According to the NCHV theory, the joint probability of any observable set exists even if the observables are not compatible pairwise.^[6,7] The difference between quantum mechanics and NCHV theory can be revealed by noncontextuality inequalities, which have different bounds in quantum and NCHV theory. For example, the KCBS inequality has the NCHV lower bound of -3 and the quantum lower bound of $5 - 4\sqrt{5}$,^[8] the CHSH inequality (it can be treated as a special type of NCHV inequalities) has the LHV upper bound of 2 and the quantum upper bound of $2\sqrt{2}$.^[6] The KCBS inequality can be simplified to the Wright inequality,^[10] which has the NCHV upper bound of 2 and the quantum upper bound of $\sqrt{5}$.

The evidence of the differences between the NCHV bound and the quantum bound of these inequalities disproves NCHV theory, showing that quantum mechanics is contextual. The contextuality of the quantum mechanics has been experimentally observed by different physical systems based on neutrons,^[11] molecular nuclear spins,^[12] ions,^[13,14] and photons.^[15–17] Recently, this concept has been

utilized in researches of quantum computation,^[18–20] quantum cryptography,^[21] and anomalous weak values.^[22]

Since there is similarity between state vectors in quantum mechanics and Jones vectors in optics, some quantum concepts and phenomena can be simulated by classical optics,^[23] such as Bell's measurement,^[24,25] entanglement,^[26,27] teleportation,^[28,29] and spin-orbit separability.^[30] Although the simulation by classical optics cannot disprove LHV theory, it can be used as a tool for visualizing abstract concepts in low-dimensional systems^[31] in optical signal processing,^[24] classical optical theory,^[24] and polarization metrology.^[26] The quantum system with multipartite degrees of freedom also can be simulated by a classical system. For example, the Hilbert space of the Bell states has a dimension of 4 . It can be realized by a quantum system with a photon pair. Each photon has two orthogonal polarization states as two degrees of freedom. On the other hand, it can be simulated by a classical optical system, which is a system with four dimensions extended by two 2-dimensional spaces of polarizations and parities.^[24,32] For the experimental observation of the quantum contextuality, since there is no space-like requirement on the experiment, it can be realized by a quantum system with a single photon, utilizing its freedoms of polarizations, paths and so on. There are also three noncontextuality inequalities that have been experimentally simulated.^[32] As a result, the joint measurement in the experiments for tests of noncontextuality inequalities can be realized by the sequential measurements.^[33] It is noticed that such quantum systems based on single photons also can be simulated by classical optical systems, which provides a way to realize the simulation of violations of noncontextuality inequalities.^[32]

*Project supported by the National Key Basic Research Program of China (Grant Nos. 2011CBA00303 and 2013CB328700) and Basic Research Foundation of Tsinghua National Laboratory for Information Science and Technology (TNList).

[†]Corresponding author. E-mail: zwei@tsinghua.edu.cn

In this paper, we investigate the classical optical simulation of violations of the Wright inequality theoretically and experimentally. The feasibility of the analogy is analyzed by descriptions of classical electrodynamics and quantum optics. Then the violation of the Wright inequality which is the simplest noncontextuality inequality, is simulated by the classical optical system. The experiment result agrees well with the theoretical analysis.

2. Wright inequality

Considering a physical system with a set of binary-value observables $\{A_1, \dots, A_n\}$, the outcome of each observable A_i is a_i , $a_i \in \{1, -1\}$. The compatibility graph which describes compatible relations of the observable set is a pentagon. In the NCHV theory, each observable A_i has a pre-determined outcome of +1 or -1 before measurements under a specific hidden variable λ . Equation (1) shows the KCBS inequality^[8] defined on this system:

$$\langle A_1 A_2 \rangle + \langle A_2 A_3 \rangle + \langle A_3 A_4 \rangle + \langle A_4 A_5 \rangle + \langle A_5 A_1 \rangle \geq -3. \quad (1)$$

Since the product of five terms in the left part of Eq. (1) is $(A_1 A_2)(A_2 A_3)(A_3 A_4)(A_4 A_5)(A_5 A_1) = (A_1 A_2 A_3 A_4 A_5)^2 = 1$, it is impossible that all the terms in

$$\{A_1 A_2, A_2 A_3, A_3 A_4, A_4 A_5, A_5 A_1\}$$

are equal to -1 simultaneously. Hence, in the NCHV theory, the lower bound of the sum of these five terms is $+1 - 1 - 1 - 1 - 1 = -3$.

To analyze Eq. (1) with the quantum mechanics, let us consider a widely used scenario, in which the observable A can be represented as $A = 2|v\rangle\langle v| - 1$. $|v_i\rangle$ and $|v_j\rangle$ are orthogonal vectors if A_i and A_j are compatible. In this scenario A_i and A_j cannot be +1 simultaneously, leading $P(A_i = 1, A_j = 1) = 0$. Hence, the term of $\langle A_i A_j \rangle$ can be simplified to

$$\begin{aligned} \langle A_i A_j \rangle &= P(A_i = 1, A_j = 1) + P(A_i = -1, A_j = -1) \\ &\quad - P(A_i = 1, A_j = -1) - P(A_i = -1, A_j = 1) \\ &= [1 - P(A_i = 1, A_j = -1) - P(A_i = -1, A_j = 1)] \\ &\quad - P(A_i = 1, A_j = -1) - P(A_i = -1, A_j = 1) \\ &= 1 - 2P(A_i = 1) - 2P(A_j = 1). \end{aligned} \quad (2)$$

As a result, the KCBS inequality Eq. (1) can be simplified to the Wright inequality,^[10]

$$\sum_{i=1}^5 P(A_i = 1) \leq 2. \quad (3)$$

However, in quantum mechanics, the upper bound of Eq. (3) can reach $\sqrt{5} = 2.24$ while the observables and the states are:

$$|\psi\rangle = [1, 0, 0]^T, \quad (4)$$

$$A_i = 2|v_i\rangle\langle v_i| - 1, \quad (1 \leq i \leq 5), \quad (5)$$

$$|v_i\rangle = \frac{1}{\sqrt{2} \sin(2\pi/5)} \left[\sqrt{\cos\left(\frac{\pi}{5}\right)}, \cos\left(i\frac{4}{5}\pi\right), \sin\left(i\frac{4}{5}\pi\right) \right]^T. \quad (6)$$

3. Simulation with a quart system by classical optics

It can be expected that the Wright inequality of Eq. (3) can be tested by a single photon. To realize the observable A_i , a quart system can be implemented. The input state, the output state and the transform matrix are

$$|\psi_{\text{in}}\rangle = \sum_{i=1}^4 a_i |i\rangle, \quad (7)$$

$$|\psi_{\text{out}}\rangle = \sum_{i=1}^4 b_i |i\rangle, \quad (8)$$

$$\hat{U} = \sum_{i=1}^4 \sum_{j=1}^4 u_{ij} |i\rangle\langle j|. \quad (9)$$

Their relation is

$$|\psi_{\text{out}}\rangle = \hat{U} |\psi_{\text{in}}\rangle. \quad (10)$$

We notice that this quart system based on single photons can be simulated by classical optical systems, which provides a way to simulate the test of the Wright inequality of Eq. (3). The classical optical system also can be demonstrated by the setup shown in Fig. 1, in which the coherent light and power meters are used.

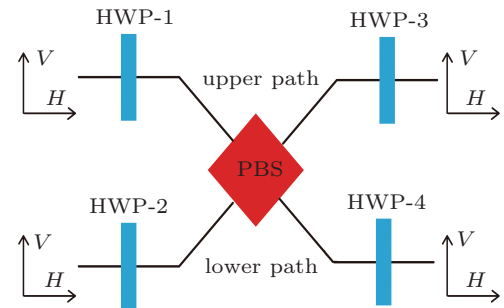


Fig. 1. (color online) A four-dimensional system consisting of a PBS and four HWPs. The four bases of the photon state are denoted by $\{|1\rangle, |2\rangle, |3\rangle, |4\rangle\}$, which are defined by their corresponding ports of $\{|U, V\rangle, |U, H\rangle, |L, V\rangle, |L, H\rangle\}$, respectively. Here, 'U' and 'L' indicate the upper path and lower path, respectively. 'V' and 'H' indicate the vertical polarization and horizontal polarization, respectively.

The input light can be represented by relation $J^{(\text{in})} = [E_1^{(\text{in})}, \dots, E_4^{(\text{in})}]^T$, while the label of $E_i^{(\text{in})}$ represents the corresponding port, corresponding to the basis of $|i\rangle$. Hence, the coherent light of $J^{(\text{in})}$ can be used to simulate any input quantum state $|\psi_{\text{in}}\rangle$ by the relation of $E_1^{(\text{in})}/a_1 = \dots = E_n^{(\text{in})}/a_n$, in which the definition of $\{a_i\}$ is from Eq. (7). In the same way, the coherent light at the output ports can be represented by $J^{(\text{out})} = [E_1^{(\text{out})}, \dots, E_4^{(\text{out})}]^T$, and the relation of $J^{(\text{out})} =$

$U * J^{(in)}$ holds. The light power measured by the power meter at the port corresponding to $|i\rangle$ is denoted by D_i , which is proportional to $E_i^{(out)*} E_i^{(out)}$. Hence, the ratio between D_i and the total power $\sum_{i=1}^n D_i$ can be expressed as:

$$\begin{aligned} \frac{D_i}{\sum_{i=1}^n D_i} &= \frac{E_i^{(out)*} E_i^{(out)}}{\sum_{i=1}^n E_i^{(out)*} E_i^{(out)}} \\ &= \frac{|[u_{i1}, \dots, u_{in}] * J_{in}|^2}{|J_{in}^T * U^T * U * J_{in}|^2} \\ &= \frac{|[u_{i1}, \dots, u_{in}] * J_{in}|^2}{J_{in}^T * J_{in}} \\ &= \left| \sum_{j=1}^n u_{ij} * a_j \right|^2 \\ &= |\langle v_i | \psi_{in} \rangle|^2. \end{aligned} \quad (11)$$

Equation (11) shows that the probabilities corresponding to the outcome of the observable A in the quantum experiment can be simulated by the measured powers in the classical optical system, which provides a simulation of the quantum experiment.

It also can be explained by the quantum mechanics description, in which the input and output lights can be expressed by coherent states of $|\phi_{in}\rangle = |\alpha_1\rangle_1 \dots |\alpha_4\rangle_4$ and $|\phi_{out}\rangle = |\beta_1\rangle_1 \dots |\beta_4\rangle_4$, respectively, in which $|\gamma\rangle_i = \exp\{\gamma \hat{a}_i^\dagger - \gamma^* \hat{a}_i\} |0\rangle$, where $\gamma \in \{\alpha_1, \alpha_2, \alpha_3, \alpha_4, \beta_1, \beta_2, \beta_3, \beta_4\}$. To simulate the states of the single photons, the relation of $\alpha_1/a_1 = \dots = \alpha_4/a_4$ should hold. The property of the system leads that $[\beta_1, \dots, \beta_4]^T = U * [\alpha_1, \dots, \alpha_4]^T$. The measured power D_i is proportional to $\langle \phi_{out} | \hat{b}_i^\dagger \hat{b}_i | \phi_{out} \rangle$, where \hat{b}_i is the annihilation operator at the i -th output port. The ratio between D_i and the

total power $\sum_{i=1}^4 D_i$ can be derived as

$$\begin{aligned} \frac{D_i}{\sum_{i=1}^n D_i} &= \frac{\langle \phi_{out} | \hat{b}_i^\dagger \hat{b}_i | \phi_{out} \rangle}{\sum_{i=1}^n \langle \phi_{out} | \hat{b}_i^\dagger \hat{b}_i | \phi_{out} \rangle} \\ &= \frac{|\beta_i|^2}{\sum_{i=1}^n |\beta_i|^2} \\ &= \frac{|[u_{i1}, \dots, u_{in}] * [\alpha_1, \dots, \alpha_n]^T|^2}{[\alpha_1, \dots, \alpha_n] * U^T * U * [\alpha_1, \dots, \alpha_n]^T} \\ &= \frac{|[u_{i1}, \dots, u_{in}] * [\alpha_1, \dots, \alpha_n]^T|^2}{[\alpha_1, \dots, \alpha_n] * [\alpha_1, \dots, \alpha_n]^T} \\ &= \left| \sum_{j=1}^n u_{ij} * a_j \right|^2 \\ &= |\langle v_i | \psi_{in} \rangle|^2, \end{aligned} \quad (12)$$

which shows the feasibility of simulating the experiment by coherent lights.

4. Experiment

An experimental ququart system consisting of a polarization-beam-splitter (PBS) and four half-wavelength-plates (HWP) is shown in Fig. 1, in which the four dimensions of the photon state are extended by the subspaces of polarizations and paths. The four bases of the photon state are denoted by $\{|1\rangle, |2\rangle, |3\rangle, |4\rangle\}$, which are defined by their corresponding ports of $\{|U, V\rangle, |U, H\rangle, |L, V\rangle, |L, H\rangle\}$, respectively. Here, 'U' and 'L' indicate the upper path and lower path, respectively. 'V' and 'H' indicate the vertical polarization and horizontal polarization, respectively. $\{\theta_1, \theta_2, \theta_3, \theta_4\}$ represent the directions of the four HWPs. The transform matrix \hat{U} in Eq. (9) is

$$\begin{pmatrix} -\sin 2\theta_1 \sin 2\theta_3 & \cos 2\theta_1 \sin 2\theta_3 & \cos 2\theta_2 \cos 2\theta_3 & \sin 2\theta_2 \cos 2\theta_3 \\ -\sin 2\theta_1 \cos 2\theta_3 & \cos 2\theta_1 \cos 2\theta_3 & -\cos 2\theta_2 \sin 2\theta_3 & -\sin 2\theta_2 \sin 2\theta_3 \\ \cos 2\theta_1 \cos 2\theta_4 & \sin 2\theta_1 \cos 2\theta_4 & -\sin 2\theta_2 \sin 2\theta_4 & \cos 2\theta_2 \sin 2\theta_4 \\ -\cos 2\theta_1 \sin 2\theta_4 & -\sin 2\theta_1 \sin 2\theta_4 & -\sin 2\theta_2 \cos 2\theta_4 & \cos 2\theta_2 \cos 2\theta_4 \end{pmatrix}. \quad (13)$$

Since this matrix \hat{U} is unitary, the four row vectors

$$|w_j\rangle = (u_{j1}, \dots, u_{j4}) \quad (1 \leq j \leq 4)$$

are normal and orthogonal pairwise. Hence, they can be utilized as the normal orthogonal bases to construct a 4-dimensional Hilbert space. $|w_1\rangle$ can be utilized to construct the observable A in the inequality by $A = 2|w_1\rangle\langle w_1| - 1$. Here, $|w_1\rangle$ is used as the eigenvector of A so that the corresponding outcome of A is $+1$. While, other vectors $|w_2\rangle, |w_3\rangle$ and $|w_4\rangle$ are eigenvectors of A so that the corresponding outcome of A is -1 . Hence, the probability of detecting the single photon at the output which corresponds to $|w_1\rangle$ is $P(A = 1)$ while the sum of the rest is $P(A = -1)$.

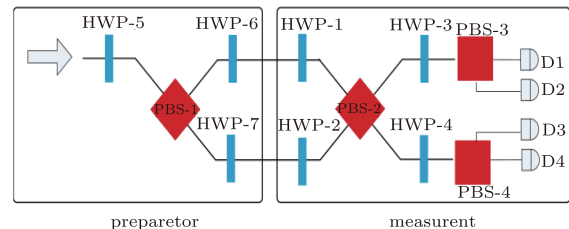


Fig. 2. (color online) Experimental simulation of violation of the Wright inequality by coherent light.

The experimental set up is shown in Fig. 2, which includes a state preparation part (left) and a measurement part (right). In the preparation part, the coherent light is generated by an HeNe laser with a center wavelength of 632.8 nm. Then

it is split to the two output ports of a polarization beam splitter (PBS1 in Fig. 2) through three half-wave plates HWP5-7. Any input state can be prepared by adjusting the directions of HWP5-7. In the measurement part, the prepared state is injected into a linear optical system as shown in Fig. 1, including one polarization beam splitter (PBS2) and four half-wave plates (HWP1-4). The output state of PBS2 is projected to the four ports by two additional polarization beam splitters

$$\{\theta_1^{(i)}, \theta_2^{(i)}, \theta_3^{(i)}, \theta_4^{(i)}\} = \left\{ -\pi/4, i2\pi/5, 1/2 \arccos\left(\frac{1}{\sqrt{2} \sin(\frac{2}{5}\pi)}\right), 0 \right\} = \{-45^\circ, i \times 72^\circ, 21^\circ, 0^\circ\} \quad (14)$$

to simulate the observable A_i shown in Eq. (5) and Eq. (6). The light powers at the four output ports of the measurement part are measured by a power meter sequentially. According to the analysis in Eq. (11) and Eq. (12), the probability $P(A_i = 1)$ can be obtained by the ratio between $D_1^{(i)}$ (the power at port 1) and the total power

$$P_i = \frac{D_1^{(i)}}{D_1^{(i)} + D_2^{(i)} + D_3^{(i)} + D_4^{(i)}}, \quad (15)$$

where $P(A_i = 1)$ is denoted by P_i .

For each P_i ($1 \leq i \leq 5$), the values of $\{D_1^{(i)}, D_2^{(i)}, D_3^{(i)}, D_4^{(i)}\}$ ($1 \leq i \leq 5$) are average results of 10 measurements, which are shown in Table 1. Then P_i is calculated, by which we can obtain the value of the left-hand side of Eq. (3). Its value is 2.17.

Table 1. Experimental result of $D_j^{(i)}$ and P_i .

i	$D_1^{(i)}/\text{mW}$	$D_2^{(i)}/\text{mW}$	$D_3^{(i)}/\text{mW}$	$D_4^{(i)}/\text{mW}$	P_i
1	0.484	0.614	0.003	0.006	0.437
2	0.482	0.604	0.005	0.017	0.435
3	0.477	0.592	0.005	0.033	0.431
4	0.482	0.615	0.005	0.008	0.434
5	0.484	0.619	0.005	0.014	0.436

On the other hand, its error should be calculated by the analysis on the measurement process of P_i . The errors of P_i (ΔP_i) have two contributions. The first one is the systematic error, which is denoted by $\Delta P_i^{(\text{sys})}$. It is determined by the precision of directions of HWPs used in the experiment, which is denoted by $\Delta \theta_j^{(i)}$. The deviations of the HWP- j directions are denoted by $\theta_j^{(i)}$ respectively, and $\Delta P_i^{(\text{sys})}$ can be calculated by

$$\begin{aligned} \Delta P_i^{(\text{sys})} &= \sqrt{\sum_{j=1}^4 \left(\frac{\partial P_i^{(\text{sys})}}{\partial \theta_j^{(i)}} \right)^2 \Delta \theta_j^{(i)2}} \\ &= 2|\sin(4\theta_3^{(i)})| \sin^2(2\theta_1^{(i)}) \Delta \theta_3^{(i)}. \end{aligned} \quad (16)$$

In the experiment, $\Delta \theta_j^{(i)}$ of all the HWPs are 1° , leading to a $\Delta P_i^{(\text{sys})}$ of 0.035.

(PBS3 ~ 4). The four ports 1 ~ 4 correspond to the four bases, respectively.

To test the Wright inequality in Eq. (3), the directions of the HWP5-7 are set as $\{\theta_5, \theta_6, \theta_7\} = \{-\pi/4, \pi/4, 0\}$. The state of the light is prepared as $[1, 0, 0, 0]^T$, leading to the light coming from the upper output port of the preparation part with vertical polarization. In the measurement part, the directions of the HWP1-4 are set as

The second contribution of the error is due to statistic errors, which is denoted by $\Delta P_i^{(\text{sta})}$. They can be calculated by the statistic errors of the 10 measurements of $D_j^{(i)}$ ($1 \leq j \leq 4$, $1 \leq i \leq 5$), which are denoted by $\Delta D_j^{(i)}$. $\Delta P_i^{(\text{sta})}$ are calculated by

$$\begin{aligned} \Delta P_i^{(\text{sta})} &= \sqrt{\sum_{j=1}^4 \left(\frac{\partial P_i^{(\text{sta})}}{\partial D_j^{(i)}} \right)^2 \Delta D_j^{(i)2}} \\ &= \frac{\sqrt{D_1^{(i)2} \left(\sum_{j=2}^4 \Delta D_j^{(i)2} \right) + \left[\sum_{j=2}^4 (D_j^{(i)}) \Delta D_j^{(i)} \right]^2}}{\left(\sum_{j=1}^4 D_j^{(i)} \right)^2}. \end{aligned} \quad (17)$$

The $\Delta D_j^{(i)}$ of the measured $D_j^{(i)}$ and calculated $\Delta P_i^{(\text{sta})}$ are listed in Table 2.

Table 2. Experimental result of $\Delta D_j^{(i)}$ and $\Delta P_i^{(\text{sta})}$.

i	$\Delta D_1^{(i)}/\text{mW}$	$\Delta D_2^{(i)}/\text{mW}$	$\Delta D_3^{(i)}/\text{mW}$	$\Delta D_4^{(i)}/\text{mW}$	$\Delta P_i^{(\text{sta})}$
1	0.0001	0.0002	0.0001	0.0001	0.0003
2	0.0001	0.0002	0.0001	0.0001	0.0002
3	0.0002	0.0001	0.0001	0.0001	0.0003
4	0.0001	0.0002	0.0001	0.0001	0.0003
5	0.0001	0.0002	0.0001	0.0001	0.0002

Finally, the error of the left-hand side of Eq. (3) is calculated by

$$\Delta = \sqrt{\sum_{i=1}^5 (|\Delta P_i^{(\text{sys})}|^2 + |\Delta P_i^{(\text{sta})}|^2)}. \quad (18)$$

Its value is 0.09.

Hence, the experimental result of the left-hand side of Eq. (3) is 2.17 ± 0.09 . It violates the noncontextuality hidden variable bound, which is 2. On the other hand, it agrees with the quantum bound, which is $\sqrt{5}$.

5. Discussion

It is worthwhile noting that the way to simulate the Wright inequality by classical light in this paper can be extended to simulating other types of noncontextuality inequalities,^[34–41] such as the Peres–Mermin inequality,^[16] state-independent-contextual inequality in qutrit,^[13] state-independent-contextual inequality in ququart,^[42] and so on. Some of these inequalities have been demonstrated by quantum optical experiments based on the measurements of single photons and also simulated by microwaves.^[32] By replacing the single photon sources and the single photon detectors with classical light sources and optical power meters, these inequalities can be simulated by classical optical experiments.

It should be noticed that although this experiment shows the violation of the Wright inequality, it is based on classical light and measurement by powermeters, hence, it cannot disprove the quantum contextuality. It is similar to the simulations of quantum phenomena by the entanglement in classical light, which is the entanglement between different degrees of freedoms.^[23] Based on classical entanglement, quantum phenomena such as the Bell measurement,^[24,25] quantum entanglement,^[26,27] and teleportation^[28,29] were simulated, visualizing these quantum phenomena in an easier way. As a basic characteristic of quantum mechanisms, contextuality is also counter-intuitive-like quantum entanglement, and the classical simulation in this experiment provides a useful tool to show it visually.

6. Conclusion

In this paper, we realize the simulation of the Wright inequality, which is the simplest form of noncontextuality inequalities, by a classical optical experiment with the coherent light. Firstly, the feasibility of the simulation is demonstrated by theoretical analysis on the physical system utilizing the descriptions of classical electrodynamics and quantum coherent state, respectively. Then, we establish the experiment setup with a laser source, free-space optical devices and optical power meters and take the measurement. The experimental results of the left side of the Wright inequality is 2.17 ± 0.09 , which violates the noncontextuality hidden variable bound of 2, while agreeing with the quantum bound of $\sqrt{5}$. The method used in this work also can be extended to other types of noncontextuality inequalities, showing that the violations of noncontextuality inequalities can be simulated by physical systems based on classical optics.

References

- [1] Einstein A, Podolsky B and Rosen N 1935 *Phys. Rev.* **47** 777
- [2] Bell J S 1964 *Physics* **1** 195
- [3] Specker E P 1960 *Dialectica* **14** 239
- [4] Kochen S and Specker E P 1967 *J. Math. Mech.* **17** 59
- [5] Bell J S 1966 *Rev. Mod. Phys.* **38** 447
- [6] Fine A 1982 *Phys. Rev. Lett.* **48** 291
- [7] Liang Y C, Spekkens R W and Wiseman H M 2011 *Phys. Rep.* **506** 1
- [8] Klyachko A A, Can M A, Binicioğlu S and Shumovsky A S 2008 *Phys. Rev. Lett.* **101** 020403
- [9] Clauser J F, Horne M A, Shimony A and Holt R A 1949 *Phys. Rev. Lett.* **23** 880
- [10] Wright R 1978 *Mathematical Foundations of Quantum Mechanics* (San Diego: Academic Press) p. 255
- [11] Hasegawa Y, Loidl R, Badurek G, Baron M and Rauch H 2006 *Phys. Rev. Lett.* **97** 230401
- [12] Moussa O, Ryan C A, Cory D G and Laflamme R 2010 *Phys. Rev. Lett.* **104** 160501
- [13] Zhang X, Um M, Zhang J, An S, Wang Y, Deng D L, Shen C, Duan L M and Kim K 2013 *Phys. Rev. Lett.* **110** 070401
- [14] Kirchmair G, Zähringer F, Gerritsma R, Kleinmann M, Gühne O, Cabello A, Blatt R and Roos C F 2003 *Nature* **460** 494
- [15] Lapkiewicz R, Li P, Schaeff C, Langford N, Ramelow S, Wiesiák M and Zeilinger A 2011 *Nature* **474** 490
- [16] Amselem E, Rådmark M, Bourennane M and Cabello A 2009 *Phys. Rev. Lett.* **103** 160405
- [17] Amselem E, Danielsen L E, López-Tarrida A J, Portillo J R, Bourennane M and Cabello A 2012 *Phys. Rev. Lett.* **108** 200405
- [18] Howard M, Wallman J, Veitch V and Emerson J 2014 *Nature* **510** 351
- [19] Raussendorf R 2013 *Phys. Rev. A* **88** 022322
- [20] Hoban M J, Campbell E T, Loukopoulos K and Browne D E 2011 *New J. Phys.* **13** 023014
- [21] Spekkens R W, Buzacott D H, Keehn A J, Toner B and Pryde G J 2009 *Phys. Rev. Lett.* **102** 010401
- [22] Pusey M F 2014 *Phys. Rev. Lett.* **113** 200401
- [23] Qian X F, Little B, Howell J C and Eberly J H 2015 *Optica* **2** 611
- [24] Kagalwala K H, Di Giuseppe G, Abouraddy A F and Saleh B E A 2012 *Nat. Photonics* **7** 72
- [25] De Zela F 2007 *Phys. Rev. A* **76** 042119
- [26] Töppel F, Aiello A, Marquardt C, Giacobino E and Leuchs G 2014 *New J. Phys.* **16** 073019
- [27] Qian X F and Eberly J H 2011 *Opt. Lett.* **36** 4110-2
- [28] Mohammad S, Rafsanjani H, Mirhosseini M, Magaña-Loaiza O S and Boyd R W 2015 *Phys. Rev. A* **92** 023827
- [29] Sun Y, Song X, Qin H, Zhang X, Yang Z and Zhang X *Sci. Rep.* **5** 9175
- [30] Borges C. V. S., Hor-Meyll M, Huguenin J A O and Khoury A Z 2010 *Phys. Rev. A* **82** 033833
- [31] Spreeuw R J C 1998 *Found. Phys.* **28** 361
- [32] Frustaglia D, Baltanas J P, Velazquez-Ahumada M C, Fernandez-Prieto A, Lujambio A, Losada V, Freire M J and Cabello A 2016 *Phys. Rev. Lett.* **116** 250404
- [33] Larsson J Å, Kleinmann M, Gühne O and Cabello A 2011 *AIP Conf. Proc.* **1327** 401
- [34] Chen X, Su H Y and Chen J L 2016 *Chin. Phys. Lett.* **33** 010302
- [35] Song X B, Wang H B, Xiong J and Zhang X D 2012 *Chin. Phys. Lett.* **29** 114214
- [36] Xiang Y and Hong F Y 2013 *Chin. Phys. B* **22** 110302
- [37] Zhang Z M 2004 *Chin. Phys. Lett.* **21** 5
- [38] Fu J and Gao S J 2008 *Chin. Phys. Lett.* **25** 2350
- [39] Zhang D Y, Xie L J, Tang S Q, Zhan X G, Chen Y H and Gao F 2010 *Chin. Phys. B* **19** 100305
- [40] Xiang Y 2011 *Chin. Phys. B* **20** 060301
- [41] Wang Y, Fan D H and Guo W J 2015 *Chin. Phys. B* **24** 084203
- [42] D'Ambrosio V, Herbauts I, Amselem E, Nagali E, Bourennane M, Sciarrino F and Cabello A 2013 *Phys. Rev. X* **3** 011012